Chapter 7

Alan Vaško [1], Mária Chalupová [2], Robert Ulewicz[3]

DEPENDANCE BETWEEN CHARGE COMPOSITION AND FATIGUE PROPERTIES OF NODULAR CAST IRONS

Abstract: The contribution deals with comparison of microstructure and fatigue properties of synthetic nodular cast irons. The basic charge of experimental meltages was formed by the different ratio of pig iron and steel scrap. The chemical composition of individual meltages was regulated alternatively by carburizer and ferrosilicon (FeSi) or metallurgical silicon carbide (SiC). The fatigue tests were run at high-frequency sinusoidal cyclic push-pull loading (frequency f ≈ 20 kHz, load ratio R = –1, temperature T = 20 ± 5 °C) using the ultrasonic testing equipment KAUP-ZU. The paper shows the influence of charge composition on microstructure, fatigue properties and micromechanisms of failure.

Key words: nodular cast iron, charge composition, microstructure, fatigue test, microfractography

7.1. Introduction

Nodular cast iron is a group of cast construction materials with a wide application in engineering practice. It combines high tensile strength and plasticity with high fatigue strength. Nodular cast iron can be produced according to the classical or synthetic casting procedure, which is more economical because cheaper steel scrap is added to the charge instead of more expensive pig iron (KONEČNÁ R. 2008). The tran-

[1] Ing. PhD., University of Žilina, Faculty of Mechanical Engineering, Department of Materials Engineering, e-mail: alan.vasko@fstroj.uniza.sk
[2] Ing., University of Žilina, Faculty of Mechanical Engineering, Department of Materials Engineering
[3] prof. P.Cz. dr hab. inż, Czestochowa University of Technology, Faculty of Management, Institute of Production Engineering

sition from the traditional use of pig iron to synthetic nodular cast iron prepared from steel scrap requires the regulation of chemical composition of melt. It is advantageous to use the metallurgical silicon carbide (SiC) as a siliconizing and carburizing additive instead of the ferrosilicon (FeSi) (VENKATESWARAN S. 1989).

The contribution deals with the influence of charge composition (i.e. different ratio of steel scrap in a charge) on the microstructure and fatigue properties of nodular cast irons. Chemical composition of individual meltages was regulated alternatively by metallurgical silicon carbide or ferrosilicon and carburizer.

7.2. Experimental material and methods

The specimens from four meltages of nodular cast iron were used for experiments. The meltages were different by charge composition (Tab. 7.1). There were 30 kg of a basic charge used for each meltage. The basic charge of individual meltages was formed by different ratio of pig iron and steel scrap and by different additive for the regulation of chemical composition. The basic charge of the meltages 3 and 8 was formed by 40 % of pig iron and 60 % of steel scrap, the basic charge of the meltages 5 and 10 was formed only by steel scrap. For the regulation of chemical composition the additive of a carburizer and metallurgical silicon carbide SiC90 was added in the meltages 3 and 5 and the additive of a carburizer and ferrosilicon FeSi75 was used in meltages 8 and 10. The content of these additives was chosen to achieve approximately the same resultant chemical composition of the meltages (eutectic degree $S_c \approx 1.2$). For modification the FeSiMg7 modifier was used and for inoculation the FeSi75 inoculant was used (VAŠKO A. 2013).

Experimental bars (diameter 32 mm and length 350 mm) were cast from all the meltages and consequently experimental specimens for tensile test, impact bending test, hardness test and fatigue tests were made (BORKOWSKI S. 2009).

Table 7.1. Charge composition of experimental meltages

Meltage number	basic charge (%)		additive
	pig iron	steel scrap	
3	40	60	carburizer + SiC90
5	0	100	
8	40	60	carburizer + FeSi75
10	0	100	

Source: own study

The metallographic analysis of specimens from experimental meltages was made by the light metallographic microscope Neophot 32. The microstructure of specimens was evaluated by STN EN ISO 945 (STN 42 0461) and by automatical image analysis using NIS Elements software (SKOČOVSKÝ P. 2007, TILLOVÁ E. 2011, BELAN J. 2013).

The fatigue tests were made by STN 42 0362 at high-frequency sinusoidal cyclic push-pull loading (frequency f ≈ 20 kHz, stress ratio R = –1, temperature T = 20 ± 5 °C) using the ultrasonic testing equipment KAUP-ZU (BOKŮVKA O. 2002, VĚCHET S. 2001, SÁGA M. 2010).

The microfractographic analysis was made by the scanning electron microscope VEGA II LMU on fracture surfaces of the specimens from experimental bars fractured by fatigue tests.

7.3. Experimental results and discussion

Metallographic analysis

From a microstructural point of view, the specimens from all the meltages are ferrite-pearlitic nodular cast irons with different content of ferrite and pearlite in a matrix, different size of graphite and count of graphitic nodules (Fig. 7.1). Different content of ferrite and pearlite in the matrix as well as different size of graphite and count of graphitic nodules in the individual specimens are caused by different ratio of steel

scrap in the charge and kind of additive for the regulation of chemical composition (SiC or FeSi).

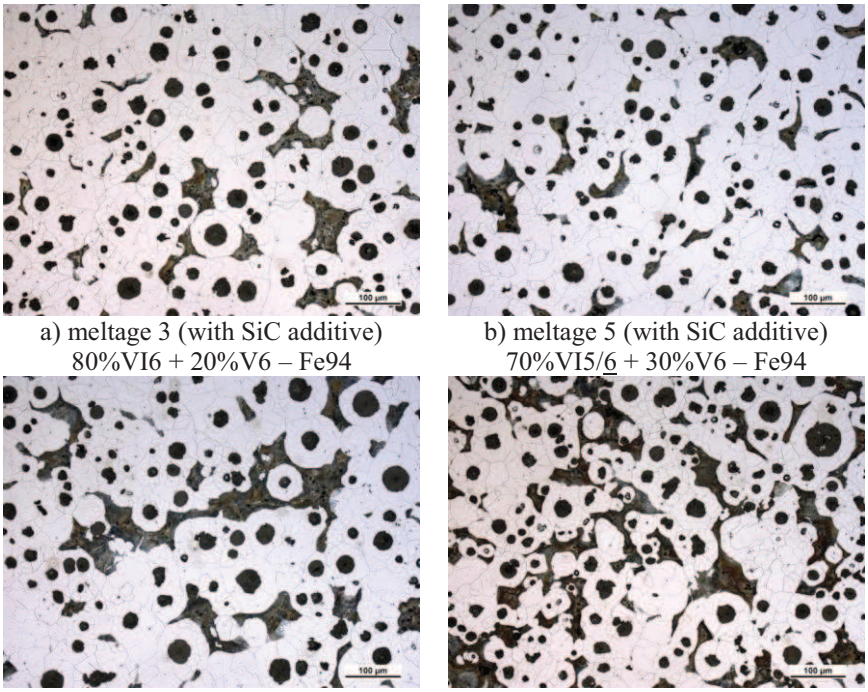

a) meltage 3 (with SiC additive) 80%VI6 + 20%V6 – Fe94

b) meltage 5 (with SiC additive) 70%VI5/6 + 30%V6 – Fe94

c) meltage 8 (with FeSi additive) 70%VI5/6 + 30%V6 – Fe80

d) meltage 10 (with FeSi additive) 70%VI5/6 + 30%V6 – Fe80

Fig. 7.1. Microstructure of the specimens from cast bars, etched 1% Nital.

Source: own study

The content of ferrite in the specimens from the meltages with SiC additive is higher than in the specimens from the meltages with FeSi additive. The highest content of ferrite was reached in the meltage 5 created only by steel scrap and SiC additive (approximately 78 %) and in the meltage 3 created by 60 % of steel scrap and SiC additive (approximately 74 %).

Graphite occurs only in a perfectly-nodular and imperfectly-nodular shape in all the specimens. The ratio of perfectly-nodular graphite in the specimens from the meltages with SiC additive is higher than in the specimens from the meltages with FeSi additive. The size of graphite is from 30 to 120 μm, but in all the specimens the size within 30-60 μm predominates. The size of graphite in the specimens from the meltages with SiC additive is generally smaller than in the specimens from the meltages with FeSi additive. The average count of graphitic nodules per unit area in the specimens from the meltages with SiC additive is higher than in the specimens from the meltages with FeSi additive. The highest count of graphitic nodules is in the meltage 3 created by 60 % of steel scrap and SiC additive (almost 200 mm^{-2}).

Mechanical properties

The mechanical tests (i.e. tensile test, impact bending test and Brinell hardness test) were realized on the specimens made from cast bars. The results of mechanical tests, i.e. tensile strength R_m, elongation A, absorbed energy K and Brinell hardness HB, are given in Tab. 7.2.

Table 7.2. Mechanical properties

Meltage number	R_m (MPa)	A (%)	K (J)	HBW 10/3000
3	539.0	4.0	30.6	192.3
5	515.7	3.7	17.2	182.3
8	462.6	2.7	24.0	181.3
10	462.6	2.7	19.2	183.0

Source: own study

The specimens from the meltages with SiC additive have better mechanical properties than the specimens from the meltages with FeSi addi-

tive. It has connection with the microstructure of the specimens, especially with the character of matrix (content of ferrite and pearlite) and also with the size and count of graphitic nodules.

The best mechanical properties were reached in the meltage 3 created by 60 % of steel scrap and SiC additive, which has the highest ratio of perfectly-nodular graphite, the smallest size of graphite and the highest count of graphitic nodules.

Fatigue properties

For the fatigue tests, ten specimens from each meltage were used to obtain Wöhler fatigue curves $\sigma_a = f(N)$ and determine fatigue strength σ_c for $N = 10^8$ cycles. The specimens were loaded by high-frequency sinusoidal cyclic push-pull loading (loading frequency $f \approx 20$ kHz).

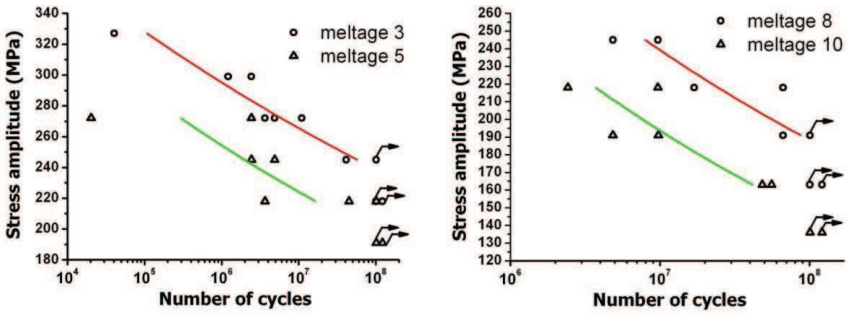

a) meltages 3 and 5 (with SiC additive)

b) meltages 8 and 10 (with FeSi additive)

Fig. 7.2. Wöhler curve $\sigma_a = f(N)$.

Source: own study

The results of fatigue tests (relationship between stress amplitude σ_a and number of cycles to failure N_f) are shown in Fig. 7.2. The number of cycles to failure increases with a decreasing stress amplitude. The values of fatigue strength σ_c are given in Tab. 7.3.

Table 7.3. Fatigue strength

Meltage number	σ_c (MPa)	Meltage number	σ_c (MPa)
3	218	**8**	163
5	191	**10**	136

Source: own study

The fatigue strength in analysed specimens of nodular cast iron increases with an increasing tensile strength.

The fatigue strength in the specimens from the meltages with SiC additive is higher than in the specimens from the meltages with FeSi additive. The highest fatigue strength (218 MPa) was reached in the meltage 3 created by 60 % of steel scrap and SiC additive, which has the best mechanical properties.

Microfractographic analysis

Three specimens from each meltage were used for the fractographic analysis of fracture surfaces after fatigue failure. The fracture surfaces of analysed specimens do not show any remarkable differences; they are characteristic of mixed mode of fracture.

The fracture surface of the specimen from the meltage 3 (with SiC additive) being loaded by stress amplitude σ_a = 272 MPa (N_f = 1.1 x 10^7 cycles) is shown in Fig. 7.3. The fatigue fracture was initiated by casting defect (Fig. 7.3a). The fatigue fracture is characteristic of intercrystalline fatigue failure of ferrite around graphitic nodules and transcrystalline fatigue failure of ferrite and pearlite in the rest of the area (Fig. 7.3b). The final rupture is characteristic of transcrystalline ductile failure of ferrite with dimple morphology (Fig. 7.3c) and transcrystalline cleavage of ferrite and pearlite with river drawing on facets (Fig. 7.3d).

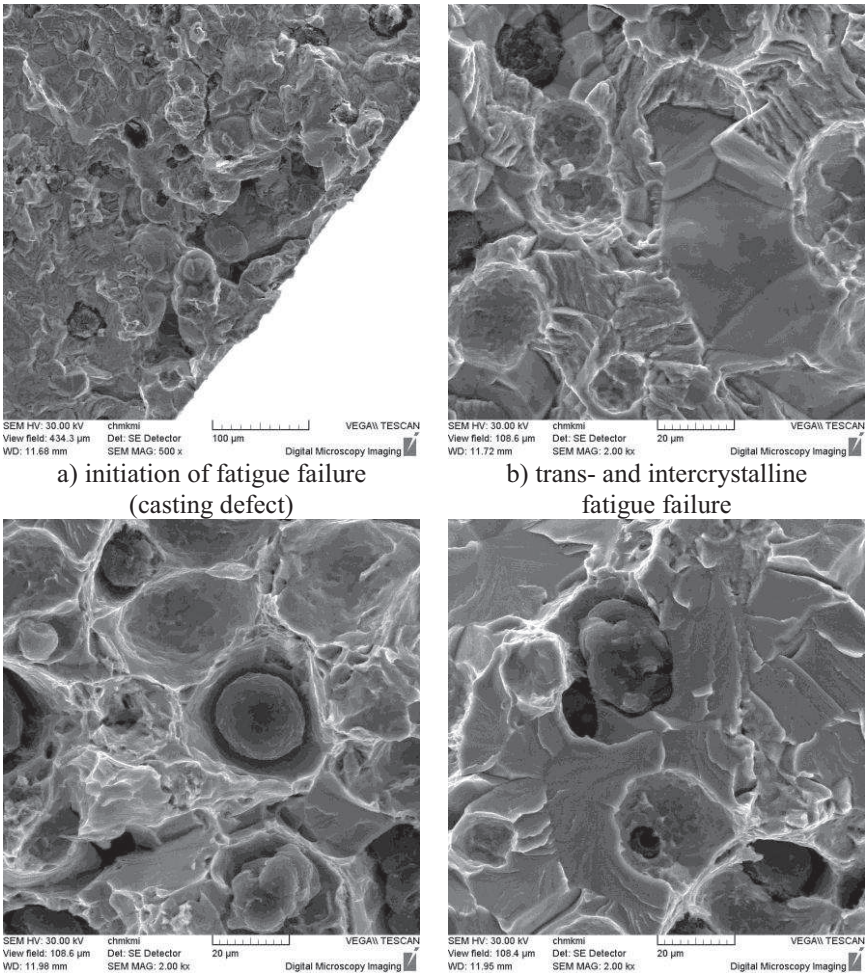

a) initiation of fatigue failure (casting defect)

b) trans- and intercrystalline fatigue failure

c) final rupture – transcrystalline ductile failure

d) final rupture – transcrystalline cleavage

Fig. 7.3. Fracture surface of the specimen from the meltage 3 (with SiC additive), σ_a = 272 MPa, N_f = 1.1 x 10^7 cycles, SEM.

Source: own study

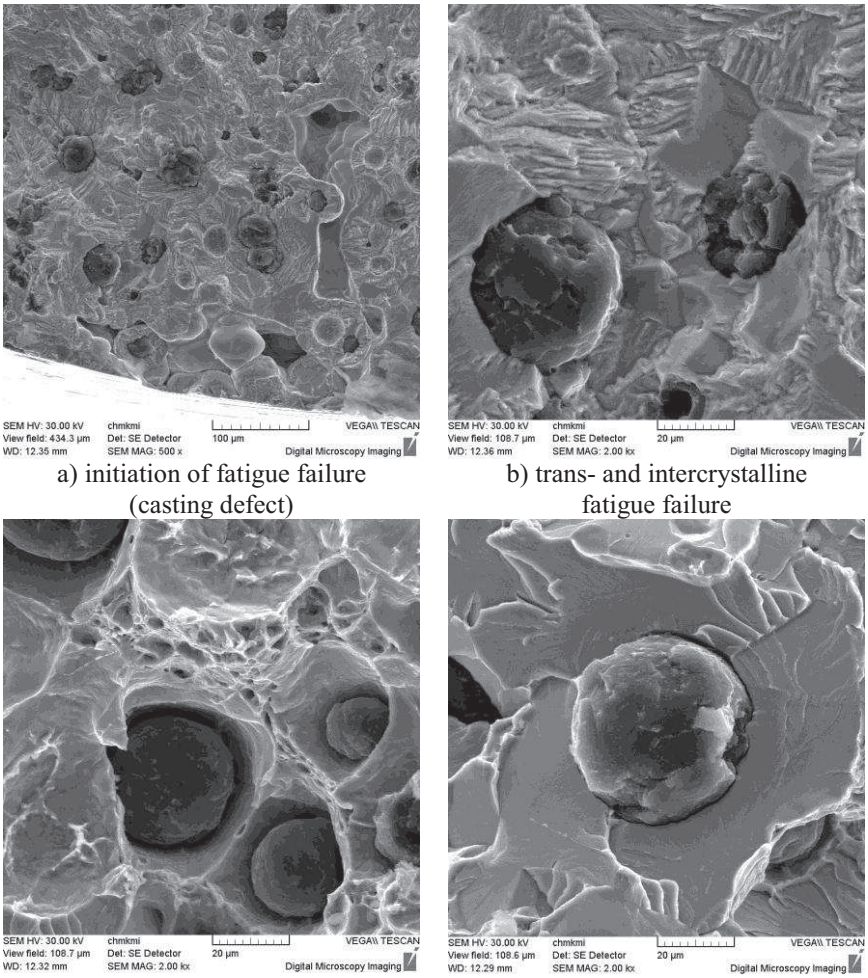

a) initiation of fatigue failure (casting defect)

b) trans- and intercrystalline fatigue failure

c) final rupture – transcrystalline ductile failure

d) final rupture – transcrystalline cleavage

Fig. 7.4. Fracture surface of the specimen from the meltage 8 (with FeSi additive), σ_a = 218 MPa, N_f = 3.0 x 10^7 cycles, SEM.

Source: own study

For comparison, Fig. 7.4 shows the fracture surface of the specimen from the meltage 8 (with FeSi additive) being loaded by stress amplitude σ_a = 218 MPa (N_f = 3.0 x 10^7 cycles). The fatigue fracture was also initiated by casting defect (Fig. 7.4a) which acted as a primary notch. The fatigue fracture is characteristic of intercrystalline fatigue failure of ferrite around graphitic nodules and transcrystalline fatigue failure of ferrite and pearlite in the rest of the area (Fig. 7.4b), similarly to the specimen from the meltage 3. The final rupture is characteristic of transcrystalline ductile failure with dimple morphology (Fig. 7.4c) and transcrystalline cleavage with river drawing on facets (Fig. 7.4d).

No significant differences were observed by the comparison of fracture surfaces of the specimens from the analysed meltages. The fatigue failure has a mixed character of fracture (intercrystalline and transcrystalline fatigue failure) in all the specimens; the intercrystalline fatigue failure predominates near graphitic nodules and the transcrystalline fatigue failure predominates in the rest of the area.

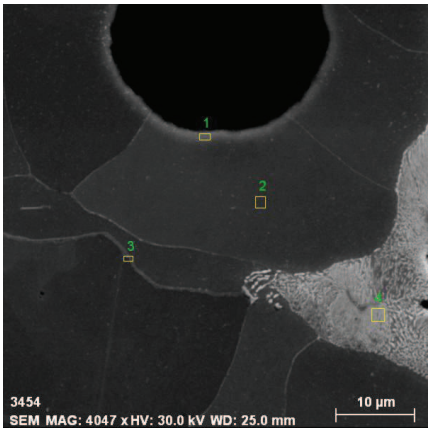

a) EDX analysis, SEM

Chemical composition (wt. %)		
position	**Si**	**Mn**
1 – ferrite near a graphitic nodule	3.78	0.35
2 – the inside of ferritic grain	3.85	0.41
3 – the boundary of ferritic grains	3.80	0.44
4 – the inside of pearlitic grain	2.34	0.95

b) results of EDX analysis

Fig. 7.5. EDX analysis of the specimen from the meltage 5 (with SiC additive).
Source: own study

Microfractographic analysis was added by EDX analysis to determine the content of silicon and manganese in the matrix (Fig. 7.5). Ferrite occuring around graphitic nodules is characterized by the high content of silicon and low content of manganese, the rest of the area (mainly pearlite) contains lower content of silicon and higher content of manganese. It explains the different micromechanisms of fatigue failure.

7.4. Conclusions

The results of the experiments show that the charge composition influences the microstructure, mechanical and fatigue properties of nodular cast iron as well as the micromechanisms of failure.

The SiC additive positively influences the microstructure, it means the content of ferrite in the matrix is increased, the size of graphite is decreased, the average count of graphitic nodules per unit area is increased and the occurrence of undesirable cementite is eliminated; consequently the mechanical and fatigue properties of nodular cast iron are improved.

The best fatigue properties (fatigue strength) from the analysed specimens has the meltage 3 created by 60 % of steel scrap and 40 % of pig iron in the basic charge with SiC additive.

Acknowledgements

This work has been supported by the Scientific Grant Agency of the Ministry of Education of Slovak Republic, grant projects VEGA No. 1/0460/11 and 1/0841/11.

Bibliography

1. BELAN J. 2013. *Study of advanced Ni-base ŽS6K alloy by quantitative metallography methods.* "Manufacturing Technology". Vol. 13, No. 1, p. 2-7.
2. BOKŮVKA O., NICOLETTO G., KUNZ L., PALČEK P., CHALUPOVÁ M. 2002. *Low & high frequency fatigue testing.* EDIS. Žilina.
3. BORKOWSKI S. – ULEWICZ R. 2009. *Laboratorium z materiałoznastwa dla inżynierów.* CWA Regina Poloniae. Częstochowa.
4. KONEČNÁ R., KONSTANTOVÁ V., NICOLETTO G. 2008. *Sizing of defects and fatigue behavior of nitrided nodular cast irons*. "Materials Science (Medžiagotyra)". Vol. 14, No. 3, p. 215-220.
5. SÁGA M., KOPAS P., VAŠKO M. 2010. *Some computational aspects of vehicle shell frames optimization subjected to fatigue life*. „Communications", Vol. 12, No. 4, p. 73-79.
6. SKOČOVSKÝ P., VAŠKO A. 2007. *Kvantitatívne hodnotenie štruktúry liatin.* EDIS. Žilina.
7. TILLOVÁ E., CHALUPOVÁ M., HURTALOVÁ L., ĎURINÍKOVÁ E. 2011. *Quality control of microstructure in recycled Al-Si cast alloys*. "Manufacturing Technology", Vol. 11, No. 11, p. 70-76.
8. VAŠKO A., TRŠKO, L., NOVÝ, F. 2013. *Fatigue resistance of syntetic nodular cast irons*. In: *Product quality improvement and companies competitiveness* (editing by BORKOWSKI S., INGALDI M.). Celje, Slovenia, p. 34-45.
9. VĚCHET S., KOHOUT J., BOKŮVKA O. 2001. *Únavové vlastnosti tvárné litiny.* EDIS. Žilina.
10. VENKATESWARAN S., WILFING J., SCHUBERT W. D., LUX B., BENECKE T. 1989. *Influence of SiC and FeSi additions on the microstructure, cooling curve and shrinkage porosity of ductile iron*. In: Physical metallurgy of cast iron. Tokyo, Japan. p. 171-178.